

# Joint analysis of low-frequency geoacoustic and deformation signals

*Mikhail Mishchenko*<sup>1,\*</sup>, *Yuriy Marapulets*<sup>1</sup>, *Igor Larionov*<sup>1</sup>, *Leonid Bogomolov*<sup>2</sup>, and *Vladimir Sychev*<sup>3</sup>.

<sup>1</sup>Institute of Cosmophysical Research and Radio Wave Propagation FEB RAS, Mirnaya, 7, Paratunka, Kamchatkskiy kray, 684034, Russia

<sup>2</sup>Institute of Marine Geology and Geophysics FEB RAS, Nauki street, 1 B, Yuzhno-Sakhalinsk, Sakhalin region, 693022, Russia

<sup>3</sup>Scientific Station RAS, Bishkek-49, 720049, Kyrgyzstan

**Abstract.** Simultaneous monitoring of signals recorded by a three-component piezoceramic seismic receiver and by a laser strainmeter-interferometer have been carried out in Kamchatka since 2016. Cases of simultaneous registration of low-frequency geoacoustic and deformation signals were detected.

## 1 Introduction

Joint monitoring of signals recorded by a three-component piezoelectric seismic receiver and a laser strainmeter-interferometer has been carried out since autumn 2016 in Kamchatka at a complex geophysical observation site “Karymshina” (52.83° N, 158.13° E) located in the zone of different-rank tectonic fracture intersection. Preliminary analysis of the data for the period 09.09.2016–22.11.2016 showed that at the background of a large number of signals received by the geophone, there are some signals recorded by the both systems. Further analysis was carried out for the data recorded from 17.10.2017 to 31.05.2018. The cases of simultaneous records of low-frequency and deformation signals were detected. Results of analysis of their time and frequency characteristics are presented.

## 2 Recording instrumentation and methods

Low-frequency geoacoustic signals were recorded by an acoustic measuring complex [1], which was developed at the Scientific Station RAS (Bishkek, Kyrgyzstan) and provided by IMGG FEB RAS within joint investigations. The measuring complex consists of two connected parts, they are: the remote and the main ones. The instrumentation remote part composed of a signal sensor and cable amplifier block is located at a signal recording point. The complex main part includes an amplification and filtration block, analog-to-digital conversion block. As a sensor for geoacoustic signals we apply a three-component piezoceramic seismic receiver A1638 developed and constructed by ZAO «Geoakustika» [2]. The seismic receiver provides transformation of acoustic signals into electric tension proportional to the oscillation acceleration in the frequency range of 0.2–400 Hz. Three orthogonal components

---

\*e-mail: [micle@ikir.ru](mailto:micle@ikir.ru)

of the oscillation acceleration are simultaneously transformed into the electric signal and they are recorded with the measurement frequency of 1 kHz. The block scheme of the acoustic measurement complex is illustrated in figure 1.

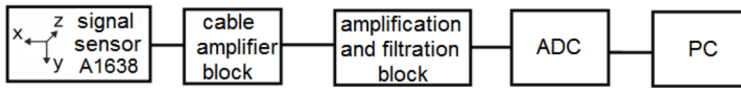


**Figure 1.** Block scheme of the acoustic measurement complex. ADC – analog-to-digital conversion block, PC – personal computer [1].

A laser strainmeter-interferometer of unequal-arm type is used to record the earth surface deformations. It was constructed according to the Michelson's interferometer scheme [3] and developed at IKIR FEB RAS. Its block scheme is shown in figure 2. It is mounted on case pipes of two five-meter dry wells spaced at 18 m (the interferometer measuring arm length). The reference arm is 0.1 m. The interferometer measuring base is covered by a wooden gallery and is South-East oriented in the direction of Kamchatka seismic focal zone. The strainmeter operation principle is that during its base change, the optical path of a laser beam, which passes the distance between two points composing the device base, changes. That entails laser radiation wave phase change due to the additional phase advance. This phase change is the measured value from which we can calculate the rock relative deformation of  $\varepsilon$ . At the output of the laser strainmeter recording system, the rock relative deformation  $\varepsilon$  is considered with the accuracy of not less than  $10^{-8}$  taking into account the meteorological parameters. The measurement frequency is 1 kHz [4]. The seismic receiver is mounted on a strainmeter optical bench end.

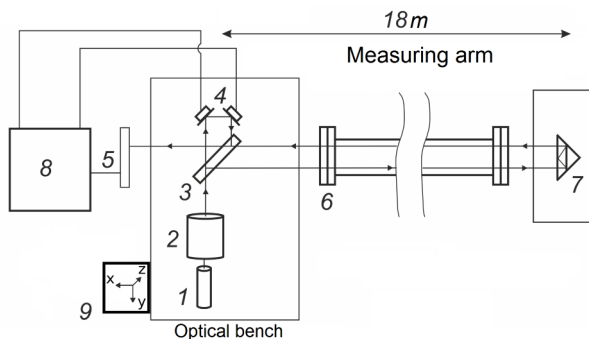


**Figure 2.** Block scheme of a laser strainmeter-interferometer. The numbers denote: 1 – laser, 2 – collimator, 3 – translucent parallel-sided plate, 4 – parallel-plane alignment mirrors on piezoceramic cylinders, 5 – photodiode, 6 – light guide, 7 – cube-corner reflector, 8 – recording system, 9 – attaching point for a three-component seismic receiver [4].

### 3 Method for signal search

The signal search is based on the data from a seismic receiver which records three components ( $x$ ,  $y$ ,  $z$ ) of oscillation acceleration vector. We considered the data for the periods of 09.09.2016–22.11.2016 and 17.10.2017–31.05.2018. The whole data massive is a sequence

of fifteen-minute files at each channel. Each file was divided into blocks with the duration of 0.2 s. After that the root-mean-square deviation (RMSD) was calculated in each block. Then a histogram of the calculated RMSD distribution was plotted. Analysis of each histogram showed that the obtained distribution is close to the normal one and the histogram maximum tends to the signal RMSD value during the background period. Then the signal to noise ratio  $SNR = \sigma_s / \sigma_f > 2.5$  was calculated for each block. If the SNR value exceeded the defined threshold value, we considered that a useful signal is present in a block. Figure 3 shows the algorithm scheme.

In the result of application of the method described above, more than 15 thousand signals with the signal to noise ratio  $SNR > 2.5$  were detected for the period under consideration. Figure 4 shows the time distribution of all the detected signals within a day. It is clear from the figure that the maximum number of signals was recorded at about 22 – 02 o'clock UTC.

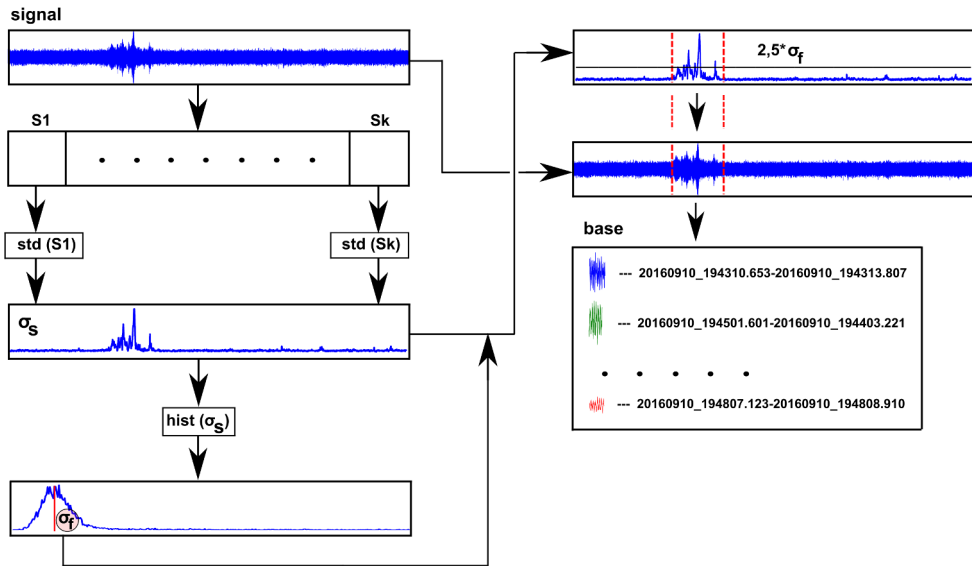


**Figure 3.** Block scheme of the algorithm for signal search.

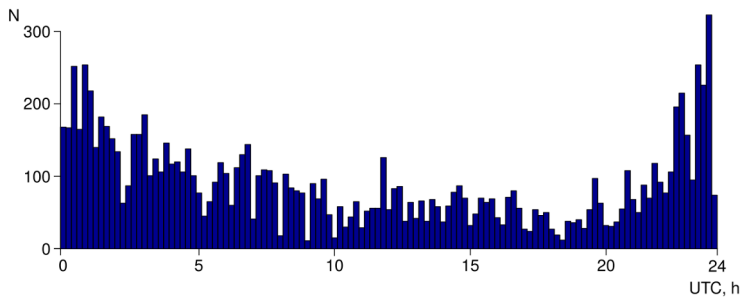
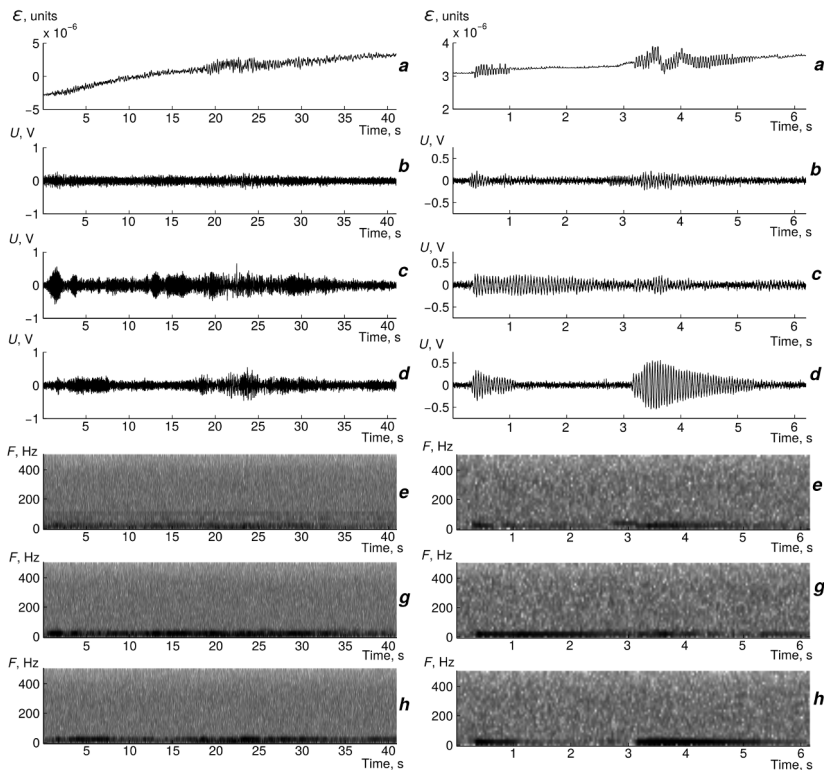


**Figure 4.** Time distribution of signals.

## 4 Results of signal analysis

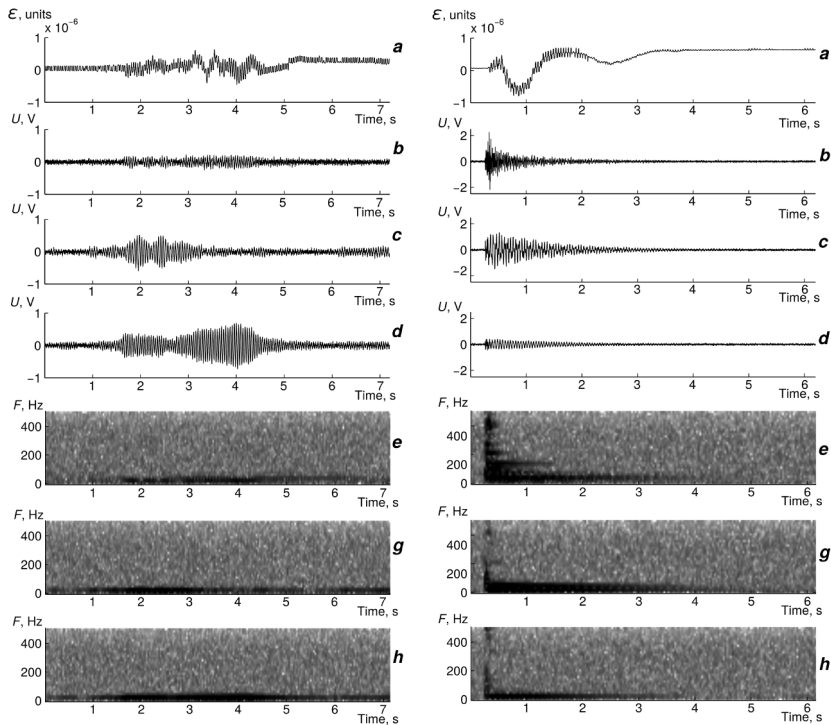
Comparison of the signals obtained from the seismic receiver with the strainmeter data showed that the majority of signals are recorded by the both systems. We can distinguish the following signals among them: seismic signals from earthquakes, anthropogenic nature signals, low-frequency geopulses, higher-frequency geoacoustic signals in the frequency range of 50–200 Hz.

Figure 5 (on the left) shows the record example of seismic event signal from “Karymshina” observation site. Earthquake characteristics: 2018.01.14, 14:04:50.3 UT, energy class is  $K_s=11.3$ , distance to the observation site is  $D=115$  km, depth is  $H=50$  km ([www.emsd.ru](http://www.emsd.ru)). Within the course of the observations, the measuring systems also recorded signals of anthropogenic origin. An example of such a signal is illustrated in Figure 5 (on the right).



**Figure 5.** Examples of records earthquake signal (on the left) and of an anthropogenic signal (on the right) by two measuring systems. For each fragment, the graphs present the following: *a* – relative deformation; *b, c, d* – three components of oscillatory acceleration vector (*z, y, x*); *e, g, h* – spectrograms of the component *z, y, x*.

Figure 6 shows the examples of recorded geoacoustic signals. To the left is a fragment with low-frequency signal (frequency is within 20–50 Hz). Signal to the right has a higher-frequency spectrum. Its frequency is estimated to be about 200 Hz.



**Figure 6.** Examples of records geoaoustic signals (on the left with the basic frequency of 20–50 Hz; to the right is the higher frequency). For each fragment, on the left and on the right of the graphs are: *a* – relative deformation; *b*, *c*, *d* – three components of oscillatory acceleration vector (*z*, *y*, *x*); *e*, *g*, *h* – spectrograms of the component *z*, *y*, *x*.

## 5 Conclusions

In the result of deformation observations that were conducted from 09.09.2016 to 11.22.016 and from 10.17.2017 to 31.05.2018, more than 15 thousand signals were detected. These signals were recorded in database. These are the signals from earthquakes, anthropogenic origin noises, low-frequency geopulses with the frequency of 50 Hz and higher-frequency geoaoustic signals in the range of 50–200 Hz. Most signals were registered by two systems simultaneously.

## References

- [1] A.S. Zakupin, L.M. Bogomolov, V.A. Mubassarova, P.V. Ilichev, *Izv-Phys. Solid Earth*, **50**(5), 692 (2014)
- [2] *Seismopriemniki p'ezoelektricheskie A16. Rukovodstvo po ekspluatatsii. 402152.004RE [Piezoelectrical seismometers A16. User manual. 402152.004RE]*, (ZAO Geoakustica, Moscow, 2006) 40
- [3] G.I. Dolgih, D.I. Valentin, S.G. Dolgih, S.N. Kovalev, I.A. Koren, V.V. Ovcharenko, V.K. Fishchenko, *Izv-Phys. Solid Earth*, **38**(8), 686 (2002)
- [4] I.A. Larionov, Yu.V. Marapulets, B.M. Shevtsov, *Solid Earth*, **5**, 1293 (2014)